Min-Max Average Pooling Based Filter for Impulse Noise Removal

Piyush Satti, Nikhil Sharma, and Bharat Garg

***Abstract*—Image corruption is a common phenomenon which occurs due to electromagnetic interference, and electric signal instabilities in a system. In this letter, a novel multi procedure Min-Max Average Pooling based Filter is proposed for removal of salt, and pepper noise that betide during transmission. The first procedure functions as a pre-processing step that activates for images with low noise corruption. In latter procedure, the noisy image is divided into two instances, and passed through multiple layers of max, and min pooling which allow restoration of intensity transitions in an image. The final procedure recombines the parallel processed images from the previous procedures, and performs average pooling to remove all residual noise. Experimental results were obtained using MATLAB software, and show that the proposed filter significantly improves edges over exiting literature. Moreover, Peak Signal to Noise Ratio was improved by 1.2 dB in de-noising of medical images corrupted by medium to high noise densities.**

***Index Terms*—Mean filters, median filters, salt and pepper noise, pooling, image restoration and de-noising.**

I. Introduction

IMPULSE noise, popularly known as Salt and Pepper (SAP) noise is introduced during acquisition and transmission phase of an image. It is defined as a sharp or sudden disturbance in input signal due to which the image pixel attain its extreme intensity values. In the last three decades, several de-noising filters were proposed to eliminate SAP noise using linear and non-linear filtering techniques. The mean or median value of the 3×3 window was used to replace the corrupted intensity. This methodology observed limited application in systems involving medium to high noise densities due to poor filter performance. Improvements in filtering methods that relied on combination and decision based techniques were introduced. These filters used a combination of mean and median which allowed better quality in medium noise densities. However, output images were observed to have high blurring effects. Further improvements were made using mathematical models like interpolation, weighted mean and probabilistic methods which boasted superior performance especially in high noise density images.

Recursive cubic Spline Interpolation Filter (RSIF) [1] is a method in which interpolation of a 3×3 window is used to determine pixel intensity, but this method is susceptible to large processing time. Moreover, weighted mean filters like Adaptive Switching Weighted Median Filter (ASWMF) [2] and Three-Value Weighted Approach (TVWA) [3] use weighted mean methods. Dynamic Adaptive Median Filter (DAMF) [4], is based on iterative techniques, however it showcases degraded performance in high noise density images. Apart from these, Fast Switching Based Median-Mean Filter (FSBMMF) [5], Switching Median and Morphological Filter (SMMF) [6] and Unbiased Weighted Mean Filter (UWMF) [7] have also been considered for a comprehensive comparative analysis.

Moreover, the advent of advanced methods inspired by artificial intelligence, machine and deep learning, remarkable improvements have been noted in image restoration processes. Classification algorithms such as support vector machines [8] and fully connected neural networks have been used to learn embedded patterns and similarity in images, this aids in restoration process with noteworthy results. The concept of Densely connected Network for Impulse Noise Removal (DNINR) [9] were also utilized. In [10], a novel two step framework is proposed where Generative Adversarial Network (GAN) and Convolution Neural Network (CNN) based blind de-noiser is used. In [11], a novel end-to-end architecture has been proposed which directly generates the de-noised image. Another CNN based approach is adopted by [12] in which five noise level CNN prior de-noisers are used. A fusion algorithm based on guided filtering is used to combine the images to obtain the noise suppressed image. Although, the results for low noise densities are impressive, these method observes catastrophic failure for higher noise densities.

In this letter, CNN inspired pooling methods have been effectively modified and used to achieve improved results, even in very high noise densities. Major contributions of the proposed work are as follows:

- Exploitation of transition in intensity values along edges of an image for utilization in impulse noise removal, a notable advantage is the difference in edge intensity level on using min vs max pooling as first layer.
- Creation and utilization of two copies of a noisy image with different pooling layer arrangements. Recombination of the different de-noised images for improved edge boundary approximations.

The rest of the paper is organized as follows. Section II presents the proposed work, with explanations for the specific choice of techniques, and the algorithm along with its various procedures. Section III enumerates the simulation results of the proposed work with comparative analysis. Finally, Section IV concludes the letter.

Manuscript received June 25, 2020; revised July 31, 2020; accepted August 4, 2020. Date of publication August 17, 2020; date of current version September 2, 2020. The associate editor coordinating the review of this manuscript and approving it for publication was Dr. Victor Sanchez *(Corresponding author: Bharat Garg.)*

The authors are with the Department of Electronics and Communication Engineering, Thapar Institute of Engineering and Technology, Patiala 147001, India (e-mail: psatti_be17@thapar.edu; nsharma1_be17@thapar.edu; bharat.garg@thapar.edu).

Digital Object Identifier 10.1109/LSP.2020.3016868

II. Proposed Work

This section presents the proposed method which utilizes pooling methods for SAP noise removal. SAP has fixed amplitude at maximum and minimum pixel intensity value. It's noise mask for an 8-bit greyscale image is given by Eq.(1), where $f(i,j)$ denotes intensity values at pixel (i,j). The noise mask stores and represents the location of corrupted pixels in an image, the value 0 identifies the pixel as a noisy pixel whereas 1 represents a noise free pixel. Noise density (N_d) of an image can also be calculated from the $noise_{mask}$ using Eq.(2), where M and N are the dimensions of the image.

$$noise_{mask}(i,j) = \begin{cases} 0 & \text{for all} f(i,j) \in \{0,255\} \\ 1 & \text{otherwise} \end{cases} \quad (1)$$

$$N_d = \frac{\sum_{i=1}^{M}\sum_{j=1}^{N} noise_{mask}(i,j)}{M \times N} \quad (2)$$

Pooling techniques are an approach used in deep learning based CNN which down samples input image into feature maps. This makes the image local translation invariant. Max, min and average pooling are the techniques used in the proposed scheme. In these techniques, pooling size and stride are two important parameters which determine quality and size of output image. It is ideal to choose pooling size as 3 (window size 3×3) due to high correlation between neighbouring pixel values and stride as 1 to preserves image dimensionality.

Further investigations have shown that a single pooling layer is insufficient for complete noise removal. It has been observed that, for a fixed 3×3 window size, a minimum of 4 pooling layers are required to remove more than 99.8% of noisy pixels, even in images corrupted by high noise densities ($>85\%$). Testing various combinations, there is a distinct improvement in using either max-min-min-max or its complementary min-max-max-min pooling layer arrangement. This is attributed to two factors: differences between the nature of max from min pooling and the amount of pixels processed by each layer.

Max pooling selects the uncorrupted brighter pixels from the window which is useful when the background of an image is dark. This also enhances lighter edges amongst dark pixels. Min pooling selects the darker intensity values and works in the opposite way. Therefore, depending upon the image and pixel being processed, one technique is better suited than the other. The percentage contribution of each layer in noise removal falls exponentially with the first layer having the highest contribution. These two factors reinforce the need for parallel processing of an image by both the max-min-min-max and min-max-max-min arrangements. The image de-noising algorithm has been broken down into three sub-procedures. Namely, Intensity Estimation for pixels with High Correlation for Lower Noise Densities (IEHCLND), Complementary Min-Max Pooling (CMMP) and a final Recombination & Smoothing step (R&S). A block-diagram has also been shown in Fig. 1, which encapsulates the proposed scheme.

Let us discuss the main algorithm. Based on noise density of the input image, the IEHCLND procedure is called which removes noisy pixels that can be estimated using surrounding intensity values. However, if the noise density is below the threshold defined, no processing is carried out. Next, two copies of the output image from the previous procedure are created.

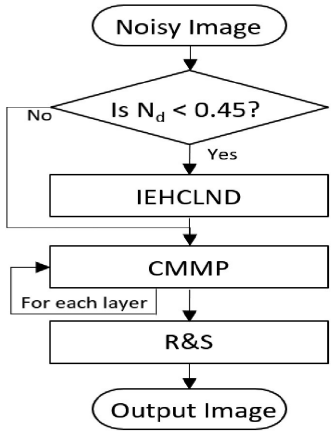

Fig. 1. Block diagram of the different procedures in the proposed work.

These copies are processed simultaneously using the CMMP procedure. Both images are rippled through the pooling layers in a pre-determined order, this step gives two output images. Finally, both images are recombined using the R&S procedure resulting in the noise free image.

A. Intensity Estimation for pixels with High Correlation for Lower Noise Densities

This procedure activates when the noise density is below 45%. If this condition is satisfied, we first calculate the window information threshold (α) using $\alpha = N_d/0.1$. Subsequently, for each noisy pixel in the image, we check its 3×3 noise free window ($W^{nf}_{3\times3}$) and store it as a list of pixel values in variable W_c. The number of elements present in the list is given by length(W_c) and also represents the number of uncorrupted pixels. If the number of uncorrupted pixels are above threshold α, we replace the corrupted pixel with its median value, otherwise no processing is done. This allows more accurate approximation of noisy pixels due to its high correlation with its surroundings.

B. Complementary Min-Max Pooling

This procedure takes two noisy images as input along with a string that decides the mode of pooling. The mode of pooling is governed by the Main algorithm. Taking the two noisy images as input, for each noisy pixel in the image, we consider a 3×3 noise free window ($W^{nf}_{3\times3}$). If the noise free window is empty, the pixel is not processed. Otherwise depending upon the string input, we either take the max-min or min-max pooling of the noise free window as replacement pixels for the first and second noisy image, respectively. Finally, the two processed images are given as output. This step is useful especially in images with frequent low to high and high to low intensity transitions.

C. Recombination & Smoothing

This procedure takes two images. In this procedure, the first operation is the pixel-wise recombination of the two images by calculation of the average intensity value. Finally, a running average pooling is performed for all corrupted pixels in the original noisy image. This results in the final noise free image. It is worth noting that the pixel-wise weighted average is not ideal for recombination as it degrades performance significantly.

Algorithm 1: MMAPF(nImg).

Input nImg ▷ *Input noisy image*
Output OutImg ▷ *Restored Image*
if $N_d < 0.45$ **then**
$I_{IEHCLND} \leftarrow$ IEHCLND(nImg)
else
$I_{IEHCLND} \leftarrow$ nImg
end if
Initialize: $I_1 \leftarrow I_{IEHCLND}, I_2 \leftarrow I_{IEHCLND}$
Initialize: $Layers \leftarrow [' Max', ' Min', ' Min', ' Max']$
for each $Layer\ in\ Layers$ **do** ▷ *Defines Pooling Layers*
[I_1, I_2] $\leftarrow$ CMMP(I_1, I_2, $Layer$)
end for
OutImg $\leftarrow$ R&S(I_1, I_2, nImg) ▷ *Recombination of images*
return OutImg

procedure IEHCLNDnImg, N_d
$\alpha = floor(\frac{N_d}{0.1})$; ▷ *Information Threshold*
for each $P_{i,j}\ in\ nImg$ **do**
$W_c \leftarrow W^{nf}_{3\times3}$ ▷ 3×3 *noise free window*
if $length(W_c) > \alpha$ **then**
$oImg_{i,j} \leftarrow median(W_c)$
else
$oImg_{i,j} \leftarrow P_{i,j}$
end if
end for
return oImg
end procedure

procedureCMMPI_1, I_2, str
Input noisy images and Layer
for each $P_{i,j}$ in I_1 **do**
$W_c \leftarrow W^{nf}_{3\times3}$ ▷ 3×3 *noise free window*
if $length(W_c) > 0$ **then**
if $str = ' Max'$ **then**
$O_1 i, j \leftarrow max(W_c), O_2 i, j \leftarrow min(W_c)$
else
$O_1 i, j \leftarrow min(W_c), O_2 i, j \leftarrow max(W_c)$
end if
end if
end for
return O_1, O_2
end procedure

procedureR&SI_1, I_2, nImg
Initialize: oImg $\leftarrow$ (I_1 + I_2)/2 ▷ *Recombination*
for each $P^{nf}_{i,j}\ in\ nImg$ **do**
$oImg_{i,j} \leftarrow$ mean($oImg^{nf}_{3\times3}$) ▷ *Average Pooling*
end for
return oImg
end procedure

TABLE I
AVERAGE PSNR VALUES OF 24 GRAYSCALE RESTORED IMAGES FROM KODAK BENCHMARK IMAGE DATASET WITH VARYING NOISE DENSITY FROM 50% TO 90%

Filter	Noise Density (%)						
	50	60	70	80	90	95	Average
ASWMF	27.20	26.07	24.96	23.77	21.89	18.66	23.76
FSBMMF	26.64	25.62	24.64	23.62	22.05	20.57	23.85
RSIF	26.15	25.17	24.15	23.07	21.5	20.12	23.36
DAMF	27.41	26.37	25.3	24.08	22.36	18.7	24.03
TVWA	28.17	27.17	25.93	24.66	22.77	21.22	24.98
SMMF	27.69	26.87	26.06	25.13	23.6	20.55	24.98
UWMF	26.93	25.94	25.06	23.91	22.61	20.39	24.14
Proposed	28.61	27.73	26.71	25.61	23.86	22.35	25.81

III. SIMULATION RESULTS

This section illustrates the performance of the proposed filter over existing algorithms. Kodak benchmark image dataset containing 24 greyscale images is used for comparing the efficiency of the algorithms. The dimensions of the images are 512×768 or 768×512. A special case, consisting of a coloured X-ray image (Lungs.png) of size 411×419 is also considered to check the productivity of the proposed algorithm in medical imaging. The noise density is varied from 10% to 95%. The results are verified using quantitative (plots and tables) and qualitative (visual representation) measures. The Peak Signal to Noise Ratio (PSNR) is calculated to substantiate the experimental results. The PSNR is defined as the ratio between the maximum possible power of the signal and the power of distorting noise. Mathematically it is given by Eq.(3) where, Max is 255 for 8-bit greyscale image. MSE is mean square error given by Eq.(4) where, M and N are dimensions of the image, $x_{i,j}$ and $y_{i,j}$ represent the pixels in the original and restored image respectively.

$$PSNR = 10log_{10}(MAX^2/MSE) \tag{3}$$

$$MSE = \frac{1}{M * N}\sum_{i=1}^{M}\sum_{j=1}^{N}(x_{i,j} - y_{i,j})^2 \tag{4}$$

The parameters used in existing algorithms are tuned as mentioned by respective authors in their research. The further subsections include simulation on Kodak benchmark image dataset and then on coloured X-ray image.

A. Experimental Results on Kodak Benchmark Image Dataset

In Table I, the average values of PSNR for the 24 grayscale images are shown with varying noise densities from 50% to 95%, and the results are plotted in Fig. 2. The proposed filter has an average improvement of around 0.85 dB over the best existing filter. At higher noise densities, the proposed filter performs exceptionally well with around 1.2 dB improvement. From the plot, we can also infer that the proposed filter has stable and consistent performance throughout the noise densities. Fig. 4(a), shows one such image from the Kodak dataset. The image is corrupted with 90% impulse noise. We can observe that Fig. 4(b) has significant quality degradation, Fig. 4(c) and Fig. 4(d) are not able to restore the image details due to the streaking effect. Fig. 4(g) and Fig. 4(h) are producing blurred restored image. Fig. 4(i) shows the restored image for the proposed filter. Here, edges of the image are preserved with relatively less blurring and low streaking effect.

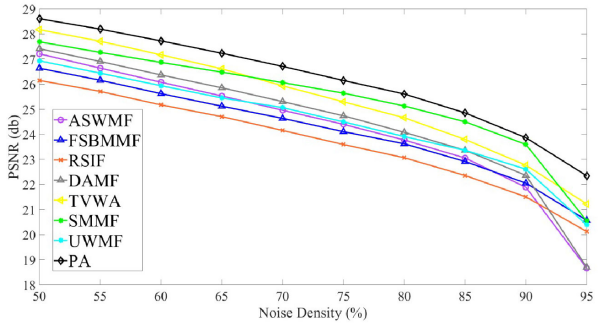

Fig. 2. Average PSNR values for Kodak Benchmark Dataset with noise density from 50% to 95%.

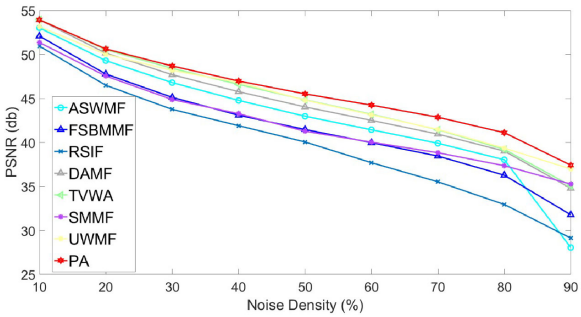

Fig. 3. PSNR values for Lungs.png with noise density from 10% to 90%

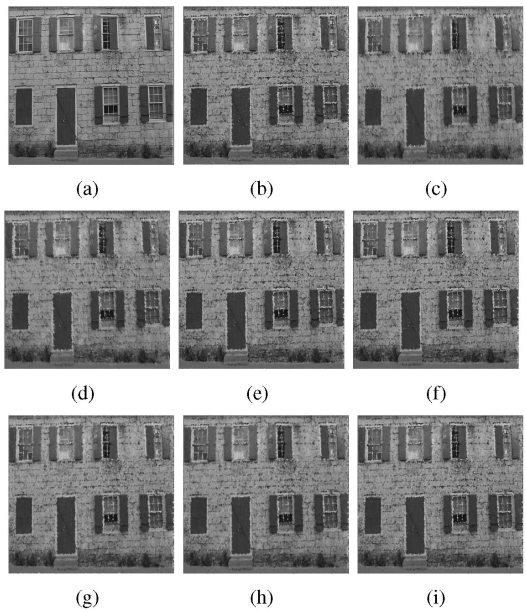

Fig. 4. (a) Original Kodak image chosen from Kodak dataset, which was filtered after 91% corruption using: (b) ASWMF, (c) FSBMMF, (d) RSIF, (e) DAMF, (f) TVWA, (g) SMMF, (h) UWMF, and (i) Proposed Filter

B. Experimental results on Coloured X-ray image

Simulation was also performed on Lungs.png with varying noise densities from 10% to 90%. PSNR values are calculated for each algorithm and the results are shown in Table II. The corresponding plot is mapped in Fig. 3. From the values, we can deduce that even for medical images the proposed filter outperforms other existing filters with an average improvement of

TABLE II
PSNR VALUES FOR DIFFERENT FILTERS ON MEDICAL IMAGE (LUNGS) FOR VARYING NOISE DENSITY FROM 10% TO 90%

Filter	Noise Density (%)					
	10	30	50	70	90	Average
ASWMF	53.03	46.8	42.98	39.91	28.06	42.16
FSBMMF	52.09	45.12	41.48	38.45	31.78	41.78
RSIF	50.96	43.76	40.05	35.53	29.13	39.89
DAMF	53.94	47.7	44.03	40.95	34.79	44.28
TVWA	53.99	48.42	44.85	41.44	35.08	44.76
SMMF	51.36	44.88	41.27	38.83	35.27	42.32
UWMF	53.16	48.18	44.81	41.48	36.99	44.92
Proposed	53.94	48.69	45.52	42.87	37.42	45.69

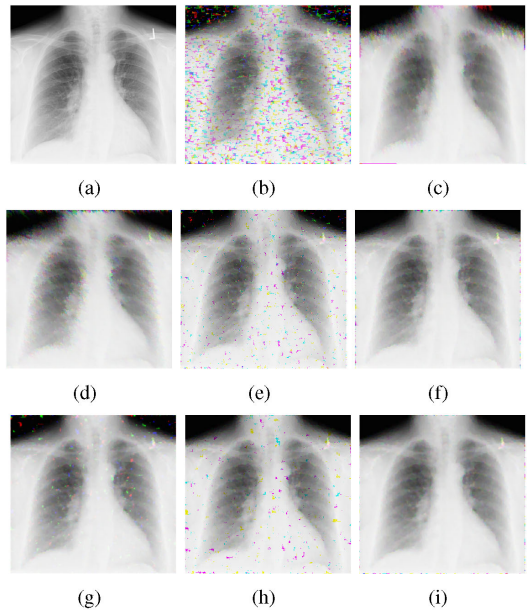

Fig. 5. (a) Original Lungs image, which was filtered after 95% corruption using: (b) ASWMF, (c) FSBMMF, (d) RSIF, (e) DAMF, (f) TVWA, (g) SMMF, (h) UWMF, and (i) Proposed Filter

1.2 dB for medium-high noise densities. Same can be concluded from the plot where the proposed filter has an better performance and margin over other existing filters. Fig. 5. shows the restored images for various filters when corrupted with 95% impulse noise. In Fig. 5 (b), (e), (g) and (h) we can see patches of irregular colours throughout the image. Fig. 5(c) and Fig. 5(d) are not able to restore the structure of the image due to blurring and streaking effects. Fig. 5(i) has the best restored results with no streaking and low blurring.

IV. CONCLUSION

In this letter, a novel Min-Max Average pooling based Filter is proposed for removal of salt and pepper noise. The proposed algorithm is divided into three procedures. The first procedure is used to improve the performance in images with lesser corruption. The second procedure splits the image into two copies and utilizes min-max pooling with different layer arrangements to capture the transitions (Bright to dark and vice-versa) in the image. The last stage performs recombination followed by average pooling operations to obtain finer edge and boundary details. Simulation results show that the proposed algorithm provides significantly improved results as compared to established literature.

REFERENCES

[1] T. Veerakumar, S. Esakkirajan, and I. Vennila, "Recursive cubic spline interpolation filter approach for the removal of high density salt-and-pepper noise," *Signal, Image Video Process.*, vol. 8, no. 1, pp. 159–168, 2014.

[2] S. Akkoul, R. Ledee, R. Leconge, and R. Harba, "A new adaptive switching median filter," *IEEE Signal Process. Lett.*, vol. 17, no. 6, pp. 587–590, Jun. 2010.

[3] C.-T. Lu, Y.-Y. Chen, L.-L. Wang, and C.-F. Chang, "Removal of salt-and-pepper noise in corrupted image using three-values-weighted approach with variable-size window," *Pattern Recognit. Lett.*, vol. 80, pp. 188–199, 2016.

[4] P. Patel, B. Majhi, B. Jena, and C. Tripathy, "Dynamic adaptive median filter (DAMF) for removal of high density impulse noise," *Int. J. Image, Graph. Signal Process.*, vol. 4, no. 11, pp. 53–62, 2012.

[5] V. Vijaykumar, G. S. Mari, and D. Ebenezer, "Fast switching based median–mean filter for high density salt and pepper noise removal," *AEU-Int. J. Electron. Commun.*, vol. 68, no. 12, pp. 1145–1155, 2014.

[6] C. Yuan and Y. Li, "Switching median and morphological filter for impulse noise removal from digital images," *Optik*, vol. 126, no. 18, pp. 1598–1601, 2015.

[7] C. Kandemir, C. Kalyoncu, and Ö. Toygar, "A weighted mean filter with spatial-bias elimination for impulse noise removal," *Digit. Signal Process.*, vol. 46, pp. 164–174, 2015.

[8] A. Roy, J. Singha, S. S. Devi, and R. H. Laskar, "Impulse noise removal using SVM classification based fuzzy filter from gray scale images," *Signal Process.*, vol. 128, pp. 262–273, 2016.

[9] G. Li, X. Xu, M. Zhang, and Q. Liu, "Densely connected network for impulse noise removal," *Pattern Anal. Appl.*, vol. 23, pp. 1–13, 2020.

[10] J. Chen, J. Chen, H. Chao, and M. Yang, "Image blind denoising with generative adversarial network based noise modeling," in *Proc. IEEE Conf. Comput. Vision Pattern Recognit.*, 2018, pp. 3155–3164.

[11] S. Zhu, G. Xu, Y. Cheng, X. Han, and Z. Wang, "BDGAN: Image blind denoising using generative adversarial networks," in *Proc. Chin. Conf. Pattern Recognit. Comput. Vision*, 2019, pp. 241–252.

[12] S. Liu, T. Liu, L. Gao, H. Li, Q. Hu, J. Zhao, and C. Wang, "Convolutional neural network and guided filtering for SAR image denoising," *Remote Sens.*, vol. 11, no. 6, pp. 1–19, 2019.